

Effects of building-induced turbulence on fluctuating suctions on roof-mounted solar arrays

*Jin-Xin Cao¹⁾, Shu-Yang Cao²⁾ and Yao-Jun Ge³⁾

^{1), 2), 3)} *State Key Laboratory of Disaster Reduction in Civil Engineering, Tongji University, Shanghai 200092, China*

¹⁾ jinxin@tongji.edu.cn

ABSTRACT

Suction loads on a single tilted solar panel on flat roofs were measured through a series of wind tunnel experiments in a boundary layer wind tunnel, using a specially-designed solar panel model. Besides wind loads, aerodynamic mechanisms which may affect extreme load events at different locations on the roof were mainly discussed, through a detailed analysis on local force spectra. For high suctions on the single tilted panel, upstream turbulence, building-induced turbulence and panel-induced turbulence are three main sources. The role of each source is different, which is depending on the location of the panel.

1. INTRODUCTION

With the rapidly increasing global use of solar photovoltaics (PV), the structural performance of such systems under environmental loads is becoming an increasingly important issue. For PV installations built into roofs (either roof-integrated or simply rooftop), wind-induced uplift loads is one of the most critical issues, and may determine the potential needs for mounting the systems. The characteristics of wind loads on rooftop solar arrays have been investigated in past decades and have attracted more attention recently. However, the basic aerodynamic mechanisms which are critical for wind load mitigation and design provision developments are still unclear (Kopp 2013). It is therefore necessary to conduct wind tunnel tests on pressure measurements on roof-mounted solar panels, which should be started from the single-panel cases.

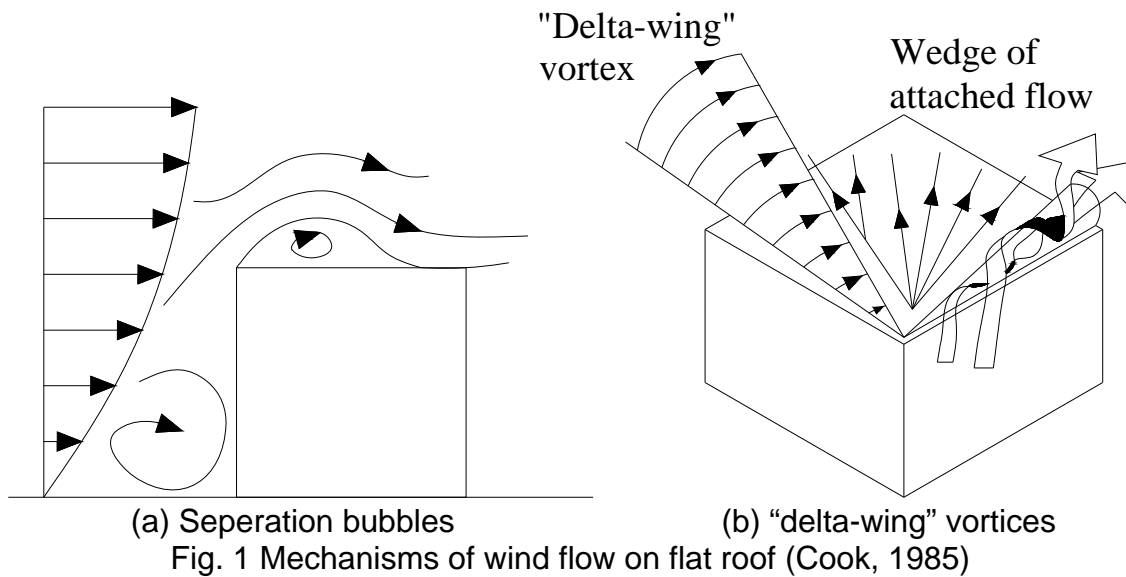
2. AERODYNAMIC MECHANISMS OF ROOF SUCTIONS

There are two mechanisms for wind flow over roofs as described by Cook (1985): separation bubble and “delta-wing” vortex, as shown in Figure 1.5a and b, resulting in high negative pressures in the separation bubble with the wind normal to the windward surface and in the “delta-wing” vortex region with the wind to be skewed at an angle of near 45 degrees to the windward surfaces.

¹⁾ Assistant Professor

²⁾ Professor

³⁾ Professor



3. EXPERIMENTAL SETUP

3.1 Pressure models

A medium-rise building model with a flat roof and dimensions of 25m (B) × 25m (D) × 20m (H) in full scale was used to support the installation of solar panel models on the roof (Fig. 1), with a geometry scale of 1:50. Considering the following investigations on the effects of building geometries on wind loads on panel modules, the building model is composed of several blocks that can be conveniently removed or installed to create varying building geometries (Fig. 2a). The solar panel model (Fig. 2b) with open substructures was 7m × 2m (14cm × 4cm in model scale), and 112 taps were installed on both upper and lower surfaces (56 taps for each) as shown in Figure 1. The pressure-tapped panel model was supported by an open frame shaped like a triangular prism that could be fixed at different locations on the building model roof. Tilt angle of 15° was considered in this study.

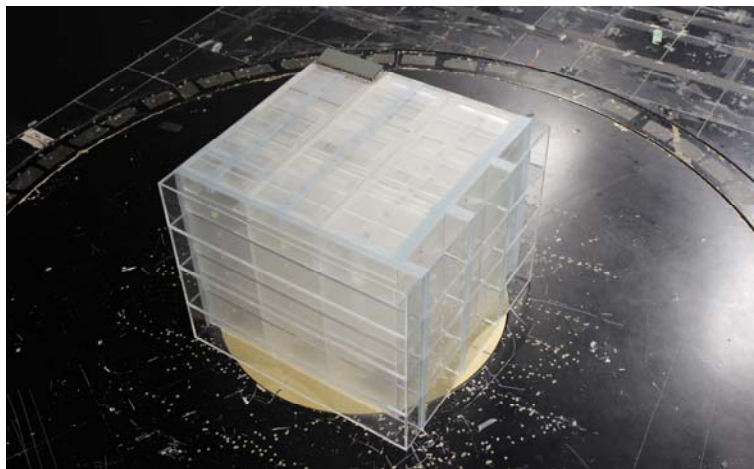
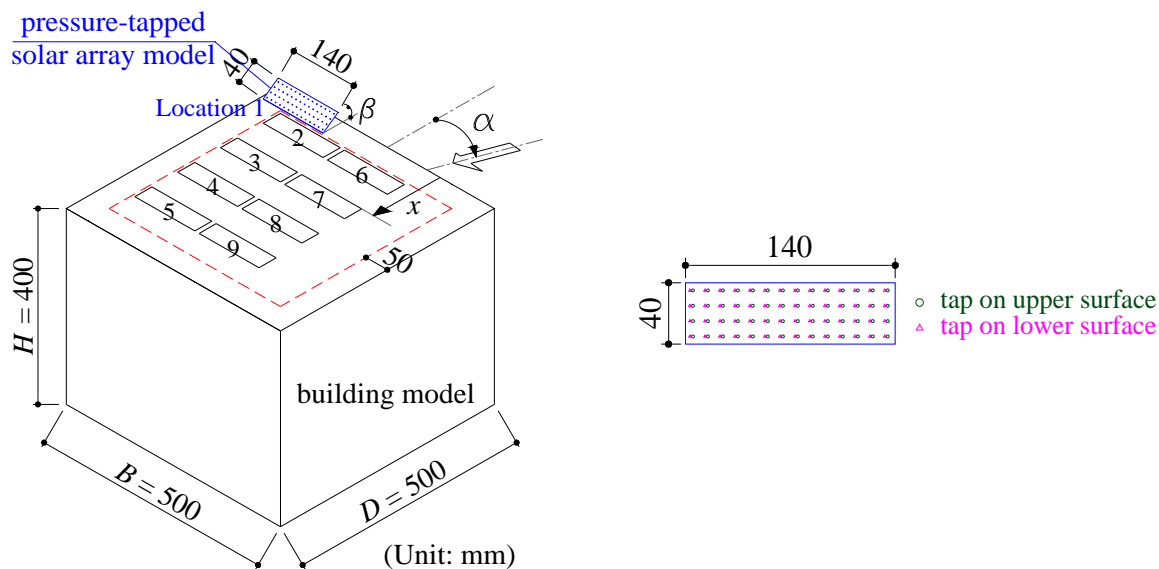


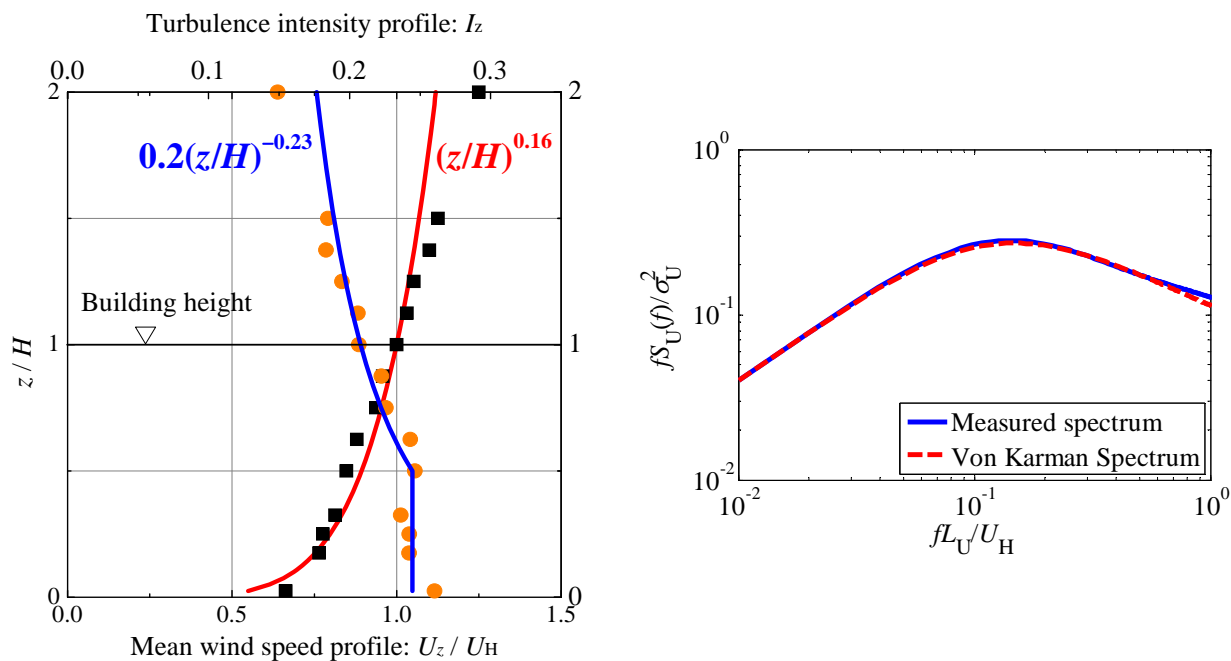
Fig. 2 Picture in wind tunnel experiment



(a) Size of experimental models

(b) Solar panel model

Fig. 3 Experimental models



(a) Profile of mean wind speed and turbulence intensity

(b) Spectrum of longitudinal turbulence

Fig. 4 Simulation of wind flow in wind tunnel

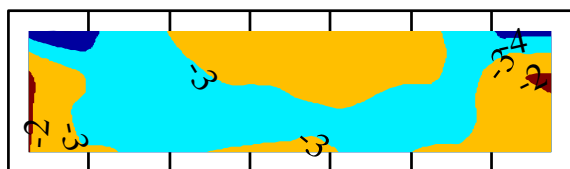
3.2 Upstream Terrain Simulation

Wind tunnel experiments were carried out in a Boundary Layer Wind Tunnel at Tokyo Polytechnic University, Japan. The test section was 2.2m wide and 1.8m high. Open terrain characteristics were simulated and a velocity scale of 1/3 was adopted. The power law exponent α of mean wind speed was 0.16. The mean wind speed at the height of the building model (400mm above the bottom of the tunnel) was 10m/s and

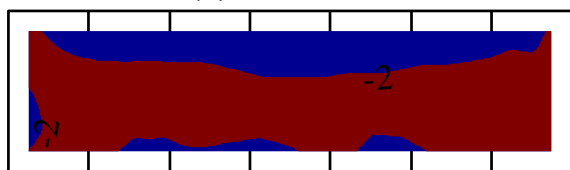
the corresponding turbulence intensity was approximately 20%, as shown in Figure 3a. The measured spectrum of longitudinal turbulence (Fig. 3b) was well agreed compared to the Von Karman spectrum.

3.3 Sampling Conditions

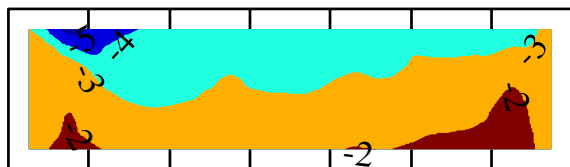
Wind pressures were acquired with a sampling frequency of 1000Hz using a multi-channel simultaneous-scanning pressure measurement system. A sampling period of 36 seconds was adopted for each data record, corresponding to 10 minutes in full scale (Time scale: 3/50). For each test case, wind directions were varied at 10° intervals and 10 data records were sampled for each wind direction. The measured pressure time histories were digitally low-pass filtered at 300 Hz. Numerical compensations were employed to correct the tube effects using the gain and phase-shift characteristics of the measurement system (Irwin 1979).



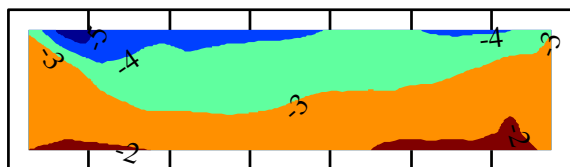
(a) Location 1



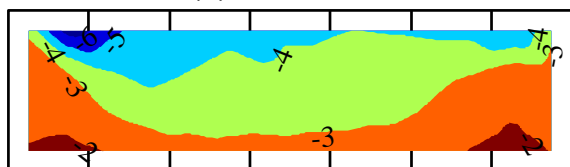
(b) Location 2



(c) Location 3

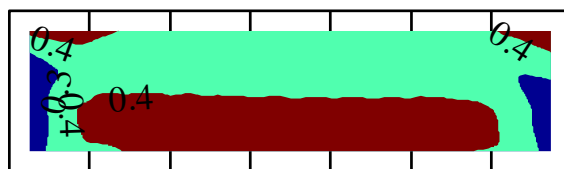


(d) Location 4

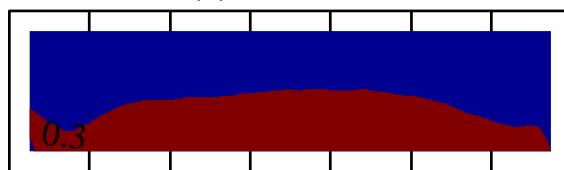


(e) Location 5

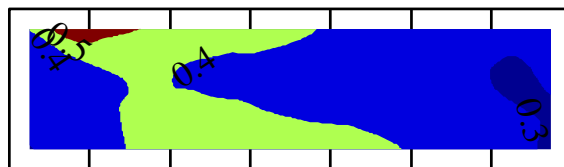
Fig. 5 Minimum local force distribution under normal wind



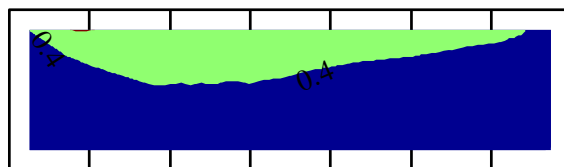
(a) Location 1



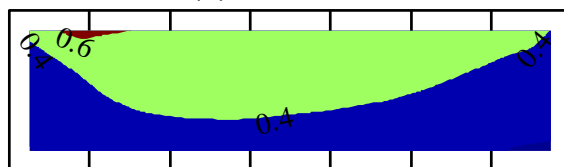
(b) Location 2



(c) Location 3



(d) Location 4



(e) Location 5

Fig. 6 Fluctuating local force distribution under normal wind

4. NORMAL WIND

For roof pressures, values decrease from the windward edge of the roof to the leeward edge under normal wind (with wind direction of 0 degree) (Cao 2012). However, variations for suction forces of the roof-mounted solar panels have different change tendencies. As shown in Figure 5, minimum local uplift forces of the tested panel (net pressures) decrease when it changed from Location 1 to Location2, and increase when it move after Location 2. Similar regulations can be found in the results of fluctuating components of local uplift forces, as shown in Figure 6. It is therefore indicated that, under normal wind, the mechanism of building-induced turbulence affecting roof pressures is different from that affecting roof-mounted solar panels.

In Figure 7, power spectra of one local force at one tap (Tap 2 among 56 taps) located at the edge of the panel model was shown, including the results when the panel moved from Location 1 to Location 5. The measured pressure spectra were presented as a function of reduced frequency, fH/U , where H is the height of the building and U is the experimental mean velocity at the height of the building. Three main peaks can be found in the spectra curves for all five locations, corresponding to the upstream turbulence, building-induced turbulence and panel-induced turbulence, respectively. These three resources of turbulence can be regarded as main factors that determine suction loads on roof-mounted solar arrays.

For different locations as shown in Figure 3a, the three resources of turbulence have different effects. For Location 1 at the windward corner, upstream turbulence played a dominant role for the fluctuating forces and the effect of building-induced turbulence can be ignored, while for Location 2, building-induced turbulence is becoming predominant and the effect of upstream turbulence is not obvious. For Location 3~5, the effects of upstream turbulence and building-induced turbulence are all comparable.

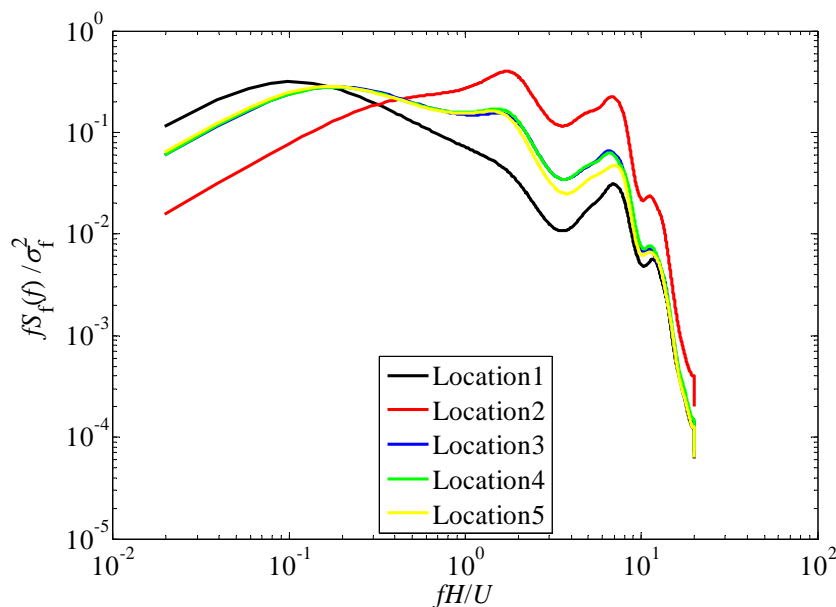
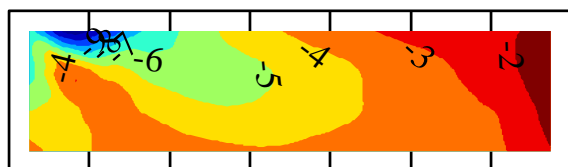


Fig. 7 Local force spectra for Tap 2 on solar panel model under normal wind

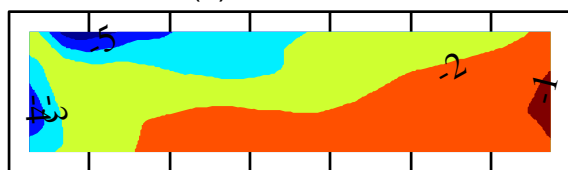
5. CORNERING WIND

Under cornering wind, high negative roof pressures were found at windward corner. Similarly, extreme suction take place at the edge of solar panel model at Location 1 under cornering wind, as shown in Figure 8. In the field of the roof, the high negative roof pressure values decrease significantly, while for the solar panel model, comparable values as that at Location 1 were found at Location 3~5. With increase in the distance from the windward edge to the panel, areas with high suction values increase, which was depicted not only in Figure 8, but also in Figure 9.

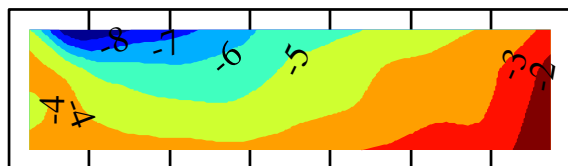
The results of force spectra in Figure 10 shows that upstream turbulence plays the most important role for Location 1 and 2, while building-induced turbulence is becoming critical for Location 3~5 where comparable high suction occur. For Location 3~5, the effect of panel-induced turbulence is also becoming obvious.



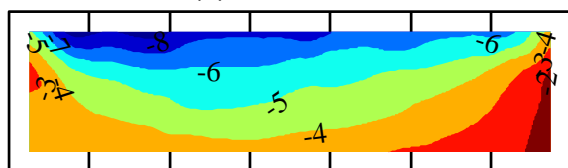
(a) Location 1



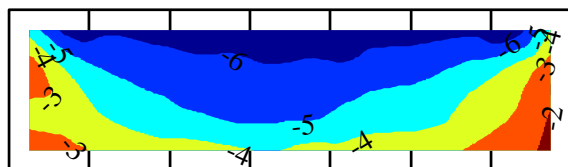
(b) Location 2



(c) Location 3

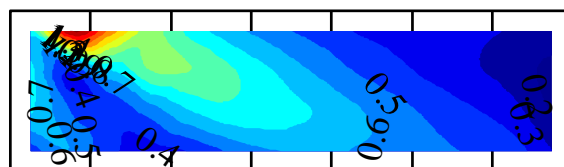


(d) Location 4

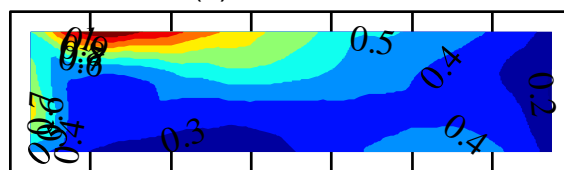


(e) Location 5

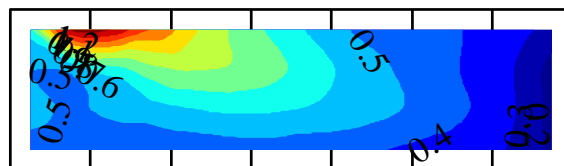
Fig. 8 Minimum local force distribution under cornering wind



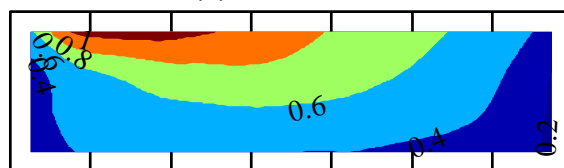
(a) Location 1



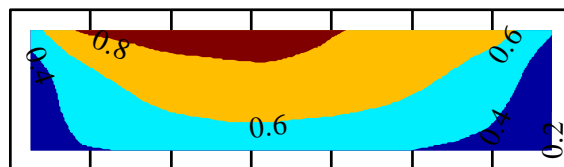
(b) Location 2



(c) Location 3



(d) Location 4



(e) Location 5

Fig. 9 Fluctuating local force distribution under cornering wind

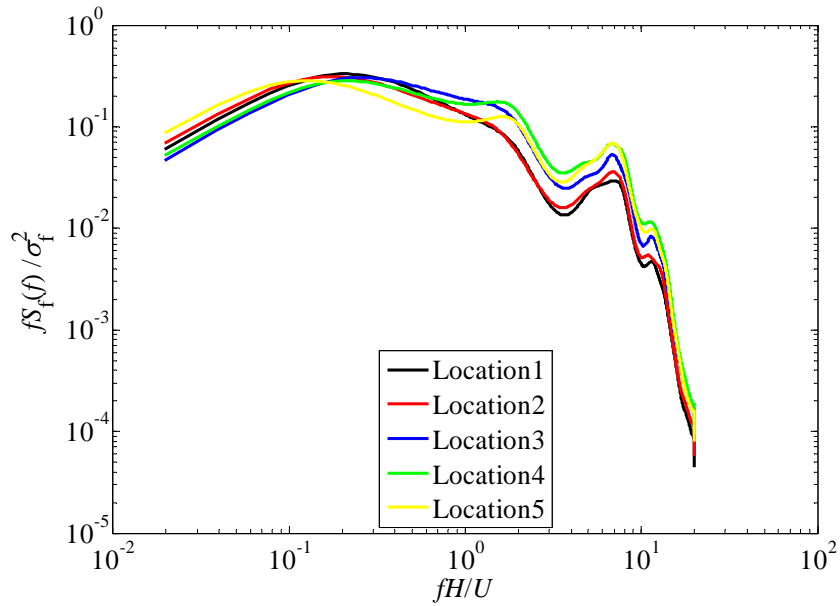
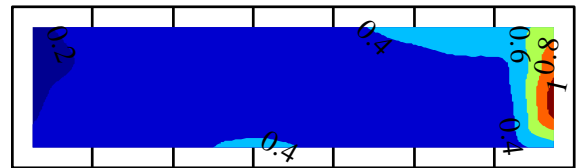


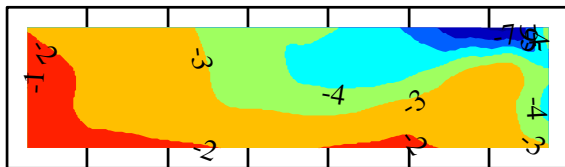
Fig. 10 Local force spectra for Tap 2 on solar panel model under cornering wind



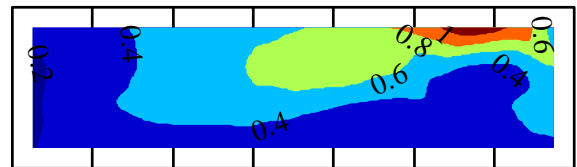
(a) Location 6



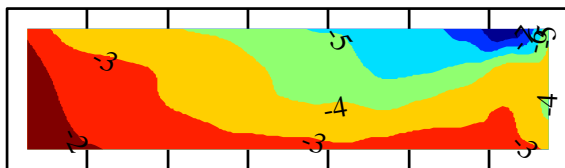
(a) Location 6



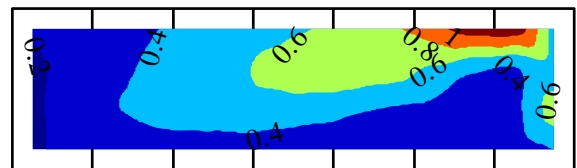
(b) Location 7



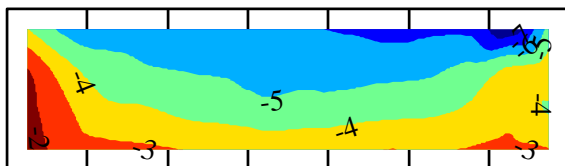
(b) Location 7



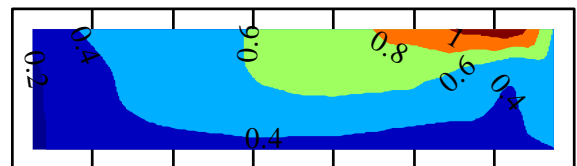
(c) Location 8



(c) Location 8



(d) Location 9



(d) Location 9

Fig. 11 Minimum local force distribution under cornering wind

Fig. 12 Fluctuating local force distribution under cornering wind

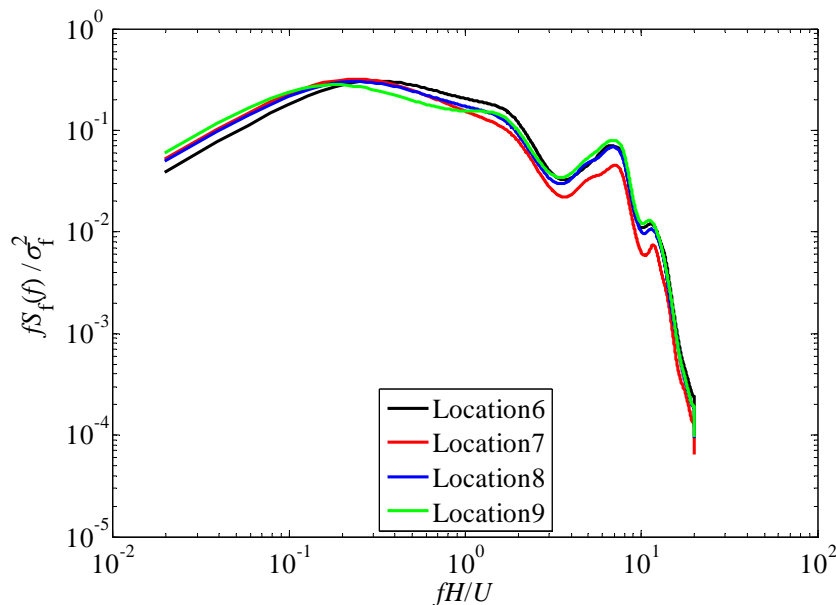


Fig. 13 Local force spectra for Tap 2 on solar panel model under cornering wind

For Location 7~9 at the central part of the roof, high suctions were recorded under cornering wind as well, as shown in Figure 11 and 12. However, negative roof pressures in these regions are extremely low compared to values at the corner. Spectra results in Figure 13 show that both upstream turbulence and building-induced turbulence affect the suction forces on the panel.

6. CONCLUSIONS

Wind pressures on both sides of a single panel mounted on a flat roof were measured through wind tunnel experiments. Regarding high suctions on the panel, three possible mechanisms were found including upstream turbulence, building-induced turbulence and panel-induced turbulence. In the regions where high roof pressures occur, upstream turbulence is most critical for panel suctions, while upstream turbulence and building-induced turbulence are both important for those regions where high roof pressures do not occur but high panel suctions are recorded. Analysis on cases with multi-arrays is needed in the future works.

ACKNOWLEDGEMENT

This study was supported by National Natural Science Foundation of China (Grant No. 51308414), Shanghai Municipal Natural Science Foundation of China (Grant No. 13ZR1462300), the Scientific Research Foundation for the Returned Overseas Chinese Scholars, State Education Ministry, and the Fundamental Research Funds for the Central Universities, which is gratefully acknowledged.

REFERENCES

- Cao, J., Tamura, Y. and Yoshida, A. (2012), "Wind pressures on multi-level flat roofs of medium-rise buildings", *J. Wind Eng. Ind. Aerodyn.*, **103**, 1-15.
- Cook, N. J. (1985), "The designer's guide to wind loading of building structures. Part 1: Background, damage survey, wind data and structural classification." Building Research Establishment, Butterworths, London, UK.
- Irwin, H.P.A.H., Cooper, K.R. and Girard, R. (1979), "Correction of distortion effects caused by tubing systems in measurements of fluctuating pressures", *J. Wind Eng. Ind. Aerodyn.*, **5**, 93-107.
- Kopp, G.A., Farquhar, S. and Morrison, M.J. (2012), "Aerodynamic mechanisms for wind loads on tilted, roof-mounted solar arrays", *J. Wind Eng. Ind. Aerodyn.*, **111**, 40-52.